# Vehicle Design Aerodynamics

## SolidWorks Flow Simulation Project Report

Warren Tie

CID: 02218280

Dyson School of Design Engineering

February 2024

# Table of Contents

# 1 Summary

Formula 1 cars represent the epitome of advanced technology in the automotive industry, showcasing the highest level of human understanding of automobiles. It is not only a sporting event but, more importantly, it has a profound and lasting impact on the mass production of cars. The constant exchange of ideas between F1 and the automotive industry has resulted in advancements in materials, fuel efficiency, and hybrid technologies.

The simulated vehicle in this study is a 1950s F1 race car. During that era, car design prioritized aggressively streamlined bodies for reduced aerodynamic drag. Investigating this vehicle not only provides a deeper understanding of early explorations in aerodynamics but also sheds light on the evolutionary history of F1.

At the beginning of the study, aerodynamic principles were applied to sketch the final concept. Then, the blueprints sketched are used to guide the construction of the CAD model. Following a preliminary estimation of the drag coefficient, a Computational Fluid Dynamics (CFD) simulation was conducted, yielding lift force at -7.278N, drag force at -260.8N, and a drag coefficient of 0.3815.

In the motorsports industry, the stability and manoeuvrability of a race car are crucial considerations. Therefore, in the improvements part, five methods have been presented primarily to enhance the car's downforce and reduce vortices. This is aimed at preventing issues such as lateral sliding, and even lifting, during high-speed acceleration, braking, and turning.

The final transformation of the car from an open-top configuration to a closed-top race car, followed by a remodelled structure and CFD analysis, resulted in a reduction in both drag coefficient and drag force. This outcome aligns with the anticipated and ideal objectives.

# 2 Sketch view of concept

## 2.1 Initial Sketch

The vehicle designed in this report is largely inspired by the Formula 1 championship car W196R from the 1950s. During the sketching process, a comprehensive examination from various angles was conducted. In order to enhance its aerodynamic performance, certain structural elements of the vehicle were refined and subsequently sketched.
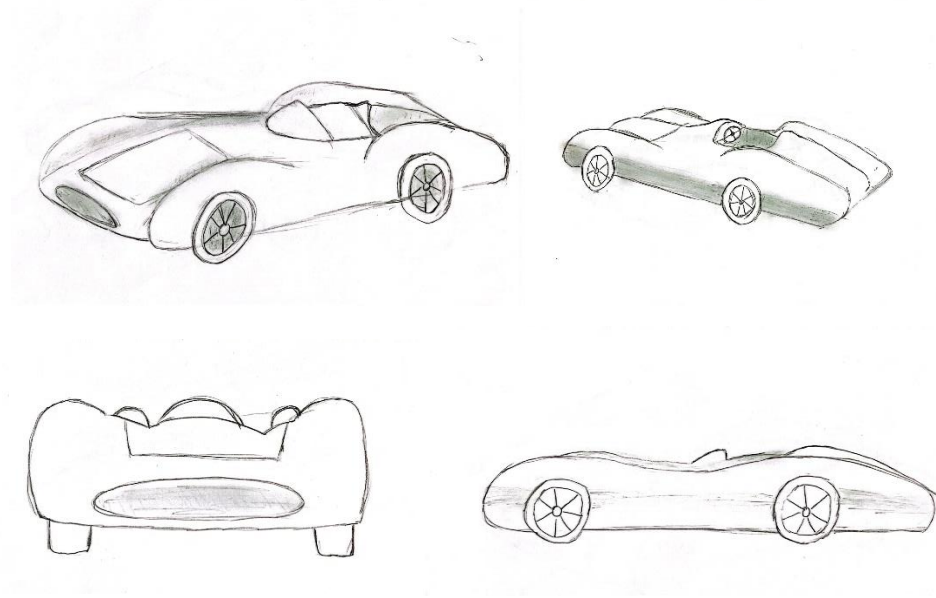


*Figure 1: Initial sketch of W196R*

## 2.2 Final Sketch

The final design adopted proportions similar to the W196R, with adjustments for optimization. Maintaining the streamlined body, enhancements like an elevated windshield and curved underbody aim to minimize drag force. Enclosed wheels reduce turbulence. The original grille design was retained for effective engine cooling.
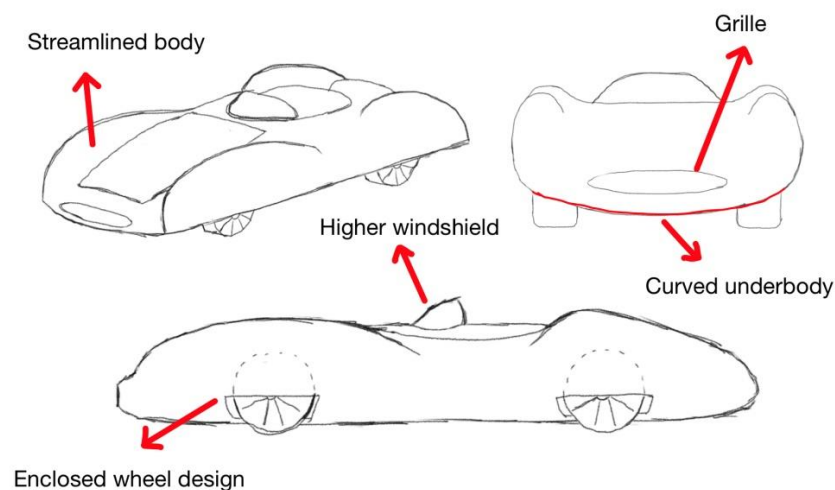


*Figure 2: Final concept and features*

# 3 CAD Model

The 3D CAD model extensively employs Surface Modelling, defining vehicle contours in both 2D and 3D using splines. Surfaces are strategically created with boundary and lofted surfaces, culminating in the final assembly through surface knitting.

Insert blueprints → Sketch using splines → Create surfaces → Knit surfaces → Model Wheels → Convert to solid body

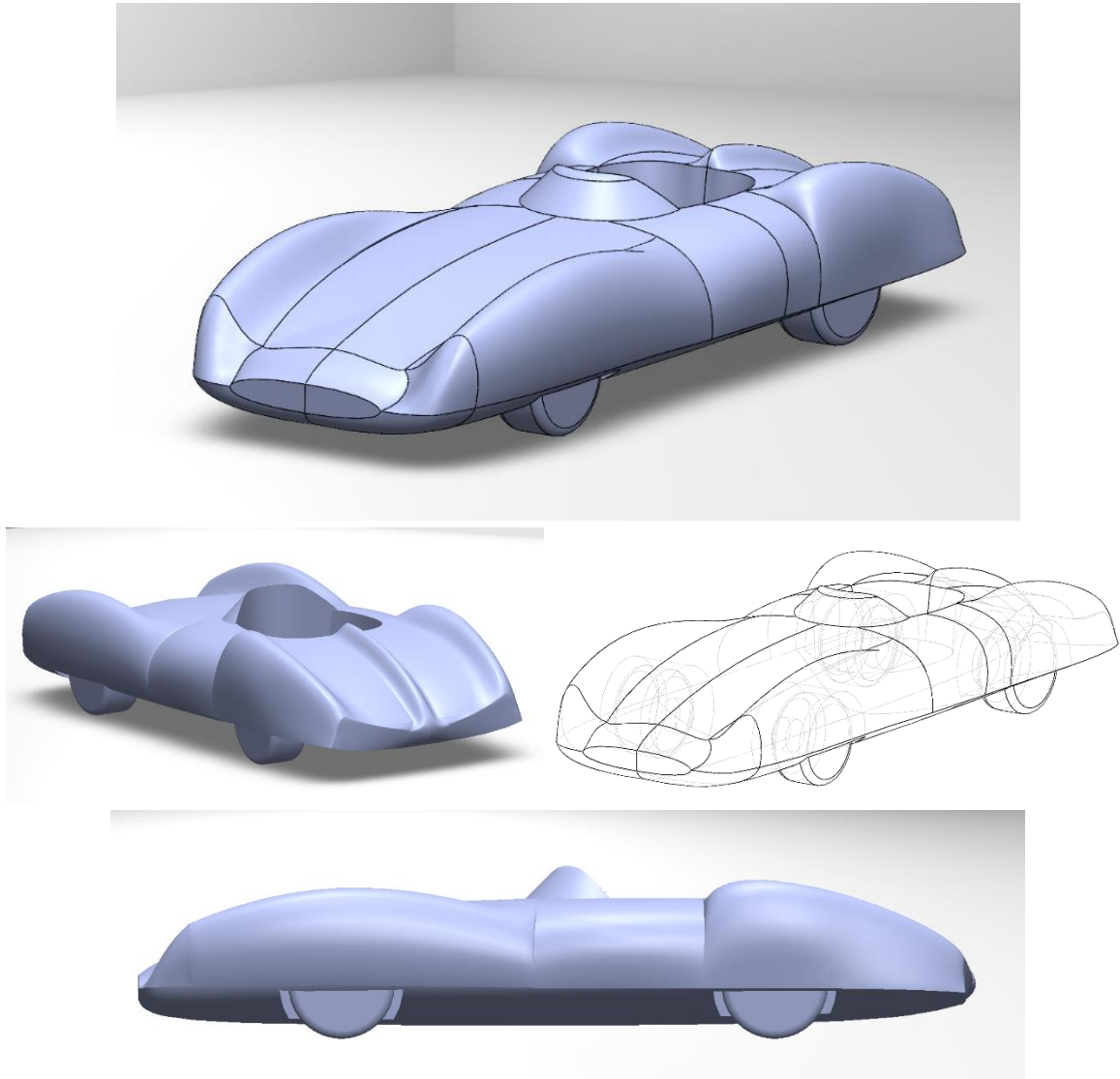*Figure 3: Rough modelling process*





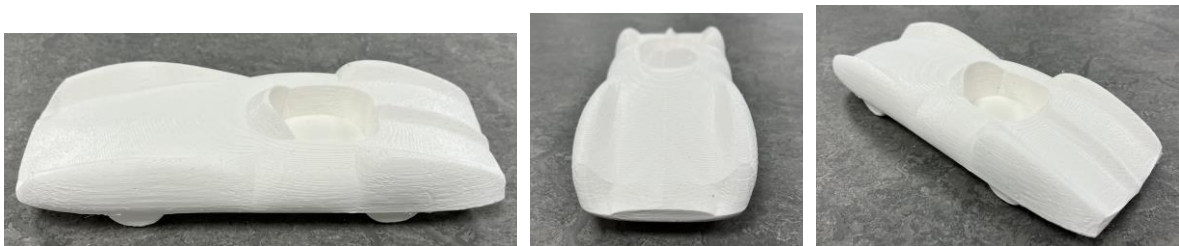*Figure 4: Low-fidelity CAD model in SolidWorks*



*Figure 5: Printed 3D model*

# 4 Preliminary Drag Analysis

The equation below can be utilized to estimate the resulting drag coefficient of the concept car:

$$C_d = 0.16 + 0.0095 \sum_{i=A}^{H} N_i$$

Where $N_i$ is a numerical value associated with a particular shape of the 8 identified car components. The corresponding $N_i$ value for each component have been summarized in Table 1.
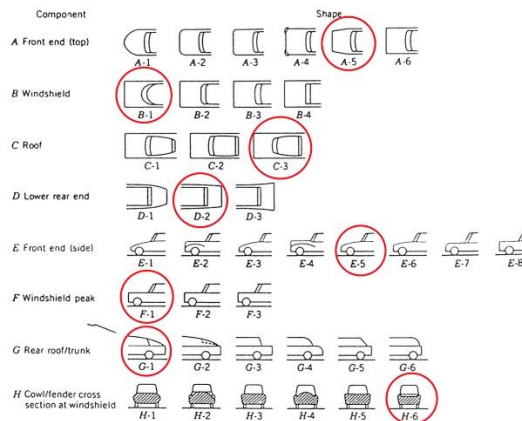


| Component | Shape | $N_i$ value |
|---|---|---|
| Front end | A-5 | 5 |
| Windshield | B-1 | 1 |
| Roof | C-3 | 3 |
| Lower rear end | D-2 | 2 |
| Front end | E-5 | 3 |
| Windshield peak | F-1 | 1 |
| Rear roof/trunk | G-1 | 1 |
| Cowl/fender cross section at windshield | H-6 | 5 |

Figure 6: Characteristics of automobile components        Table 1: $N_i$ values of automobile components

$$C_d = 0.16 + 0.0095(5 + 1 + 3 + 2 + 3 + 1 + 1 + 5)$$
$$\boldsymbol{C_d = 0.3595}$$

The estimation presented is not highly accurate. Due to the nature of the concept car being a race car, it proves challenging to identify analogous component features from Figure 6. For instance, the concept car is a convertible, thus it lacks a roof.
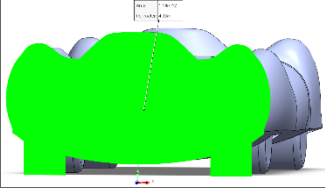
# 5 CFD Analysis

## 5.1 Values and Settings [1]

| Vehicle Data | Frontal Area: 1.14m^2 |
| --- | --- |
|  |  |
| Analysis of Mesh | Total Cell Count: 771309<br>Fluid Cells: 771309<br>Fluid Cells contacting solids: 78731<br>Iterations: 201<br>CPU time: 744 s<br>Resolution level: 7 |
| Physical Calculation Options | **Velocity Parameters:**<br>   Velocity in X direction: 0 m/s<br>   Velocity in Y direction: 0 m/s<br>   Velocity in Z direction: -31.29m/s<br>**Turbulence Parameters:**<br>   Intensity: 0.10%<br>   Length: 0.020 m<br>**Thermodynamic Parameters:**<br>   Static Pressure: 101325Pa<br>   Temperature: 293.2K<br>**Material:**<br>   Fluids: Air<br>**Wall Conditions:**<br>   Adiabatic Wall<br>   Roughness: 0 |

*Table 2: Values and settings*

## 5.2 Drag Calculation

The drag coefficient is typically computed using the following formula:

$$C_D = \frac{2F_D}{\rho A v^2}$$

Where, F is the GG Force (Z), the $\rho$ is the density of the air which is 1.225 ($kg/m^3$), A is the Frontal Area which is $1.14m^2$, and the $v$ is the velocity in Z direction which is -31.29 $m/s$.

In Equation Goal, type the formula ((2*{GG Force (Z) 2})/(1.225*979.06*1.14))*(-1). Multiplying by -1 ensures $C_D$ stays positive and is not affected by negative Z-direction velocity.

| Goal Name | Unit | Value | Progress | Use In Convergence | Delta | Criteria |
|-----------|------|-------|----------|--------------------|-------|----------|
| Lift Force | [N] | -7.278 | 100 | Yes | 15.33 | 15.82 |
| Drag Force | [N] | -260.8 | 100 | Yes | 3.748 | 33.26 |
| Drag Coefficient | [] | 0.3815 | 100 | Yes | 0.0055 | 0.0487 |

*Table 3: Results from Goal Plot*

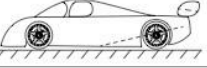**Calculated Drag Coefficient ($C_D$): 0.3815**



*Figure 7:* Range of the lift and drag coefficients (based on frontal area) for generic ground vehicle shapes. *[2]*

The $C_D$ calculated through CFD is relatively close to the initially estimated value. The shape of the concept car appears similar to the "low drag vehicle near the ground" in Figure 7, but the $C_D$ of the concept car is significantly higher than the displayed value of 0.15. This disparity may be attributed to the characteristics of the open-top design, where airflow does not fully touch the vehicle but instead flows towards the cabin, creating vortices and increasing drag.

The car's flat shape limits the pressure difference between the roof and the underbody, resulting in small upward lift during high-speed travel and generating downforce of 7.278N. The downforce enhances the car's stability, reducing the likelihood of sliding during high-speed acceleration, braking, and turning, it may also contribute to increased drag.
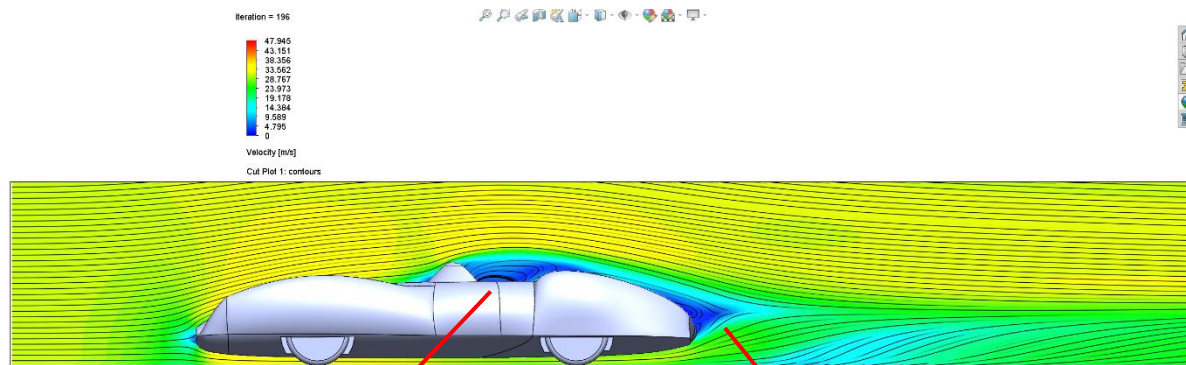
## 5.3 2D Velocity Plot



*Figure 8: 2D velocity plot*

Significant flow separation has occurred at the rear of the car, likely due to the bluff body shape of the vehicle. The abrupt change in the shape of the vehicle's rear can result in airflow detachment from the surface. Due to the insufficient height of the car's windshield, a portion of the air, after being lifted, reattaches to the vehicle surface, entering the cabin. This continuous flow within the cabin results in significant turbulences as the plot shows. The velocitiy difference between the upper and lower surfaces of the vehicle is small, which is one of the main reasons for the downforce.
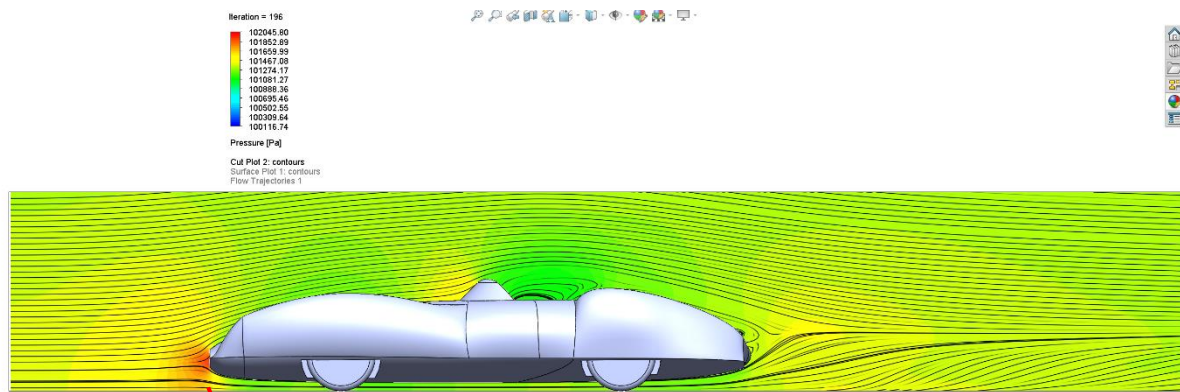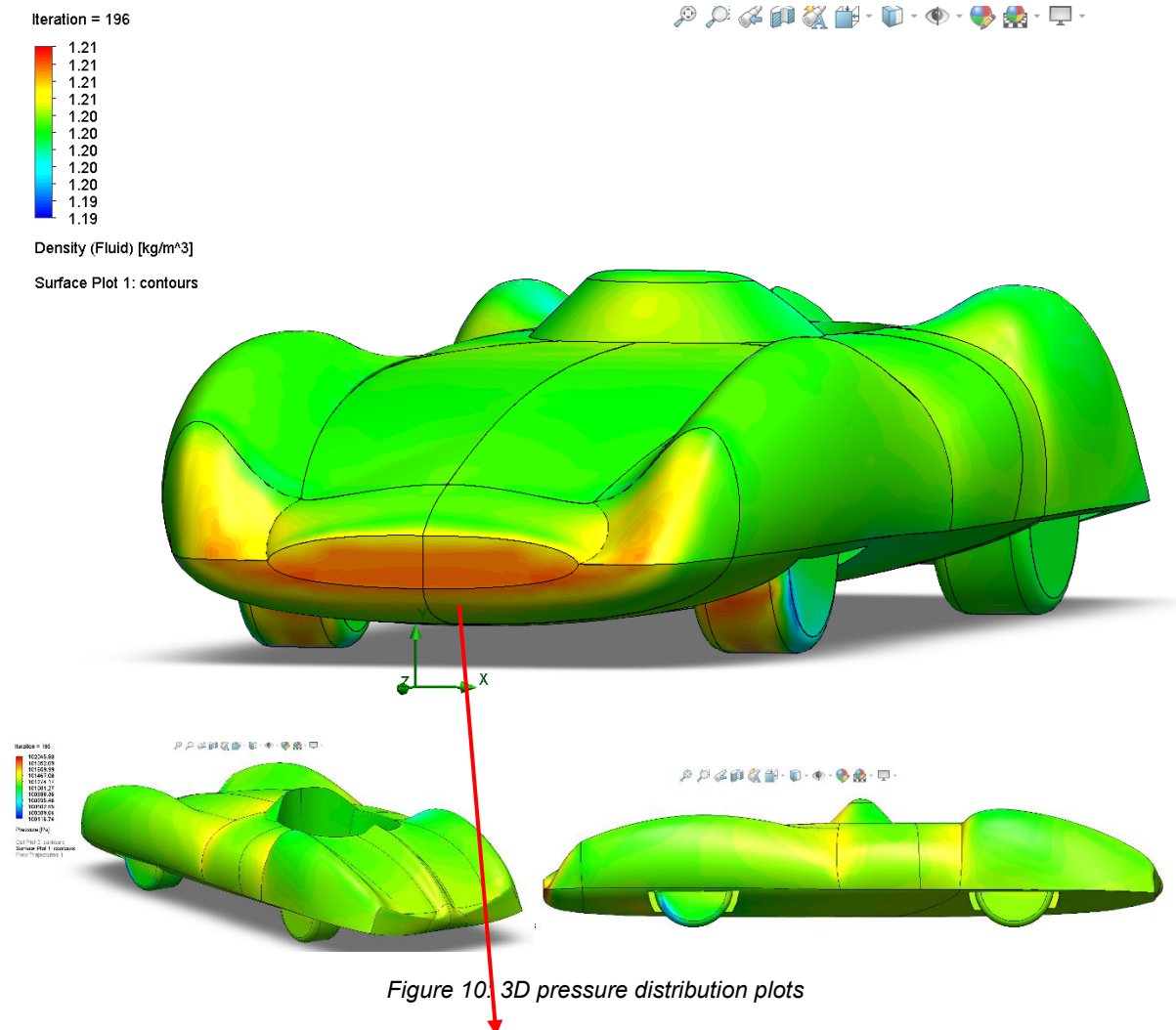
## 5.4 2D Pressure Plot



*Figure 9: 2D pressure plot*

According to this figure and the previous discussion, there is a quite small pressure difference between the roof and underbody, but a high-pressure zone is generated at the car's engine shield, which contradicts the concept of low drag. However, in actual circumstances, this area is allowed for the air to pass through for engine cooling, therefore, the frontal pressure is not very high, and as a result, it does not lead to excessive pressure and large drag.

## 5.5 3D Pressure Distribution Plot



*Figure 10. 3D pressure distribution plots*

Similar to the 2D pressure plot, the overall pressure distribution on the car body is relatively uniform, but high-pressure regions are observed near the engine shield and the front face of the front wheels. As mentioned earlier, when the engine shield is hollowed out to serve as an air channel, the issue of high-pressure zones can be addressed.

## 5.6 3D Flow Trajectories

*Figure 11: 3D flow trajectories*
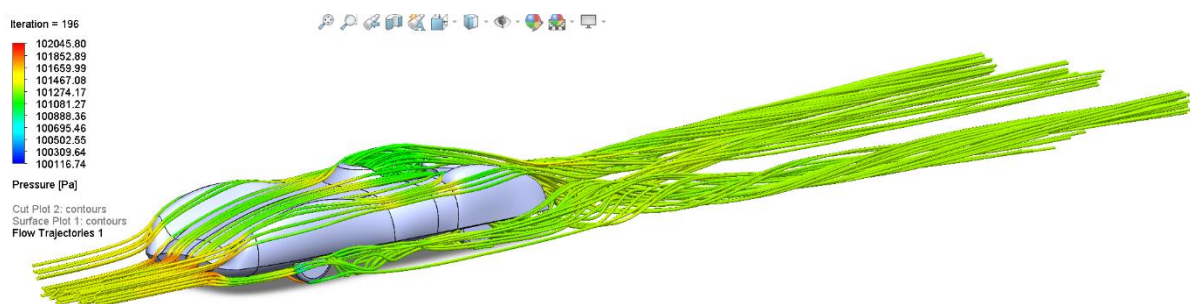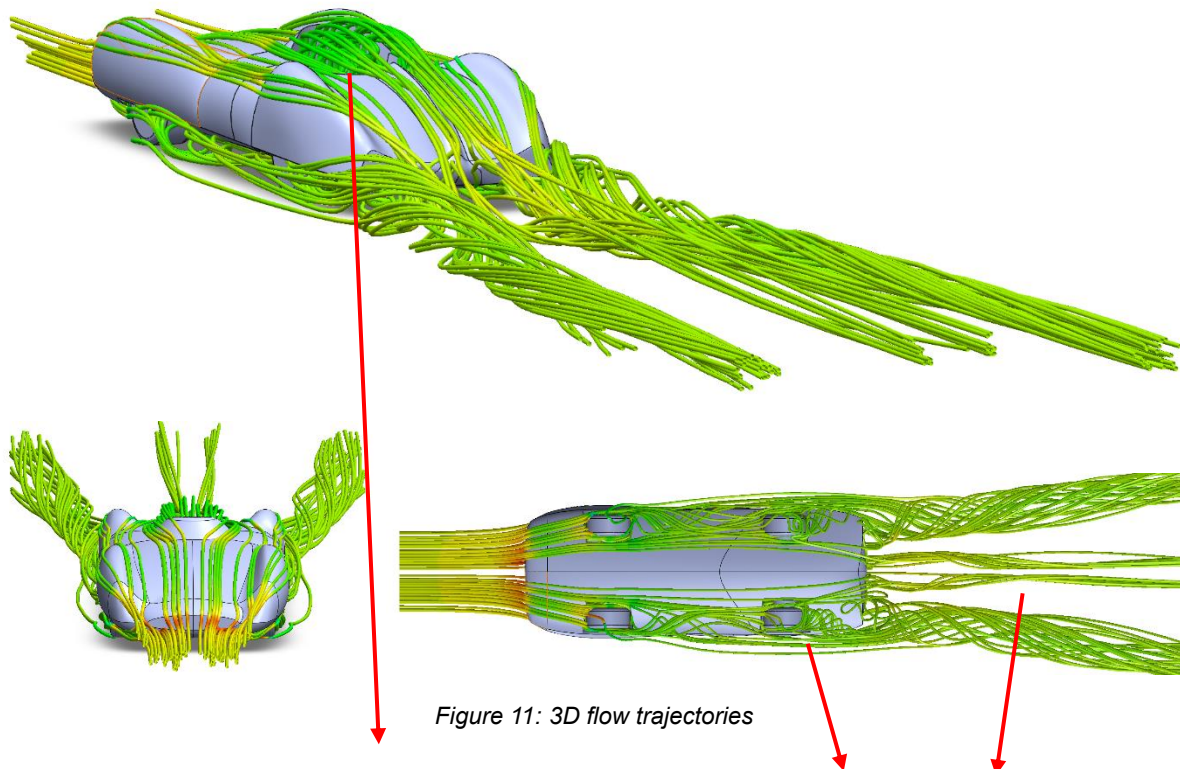
Due to the curvature of the underbody, air ingress into the wheel arches generates considerable turbulence. The three bluff body structures at the rear of the car, characterized by abrupt changes in shape, split the airflow into three turbulent streams, leading to several low-pressure zones at the rear. This contributes to large drag forces, affecting the overall aerodynamic performance of the race car. Resolving the turbulence formed within the cabin presents a subsequent challenge that needs attention.

# 6 Discussion-Wind Tunnel Test

In order to ensure the validity of CFD results, it is crucial to compare them with real-world data. A sports car was designed, 3D printed and tested in a wind tunnel. Compare the two cars and discuss the differences observed, aiming to further validate the overall CFD outcome. [3]
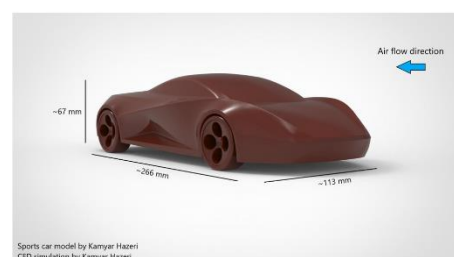


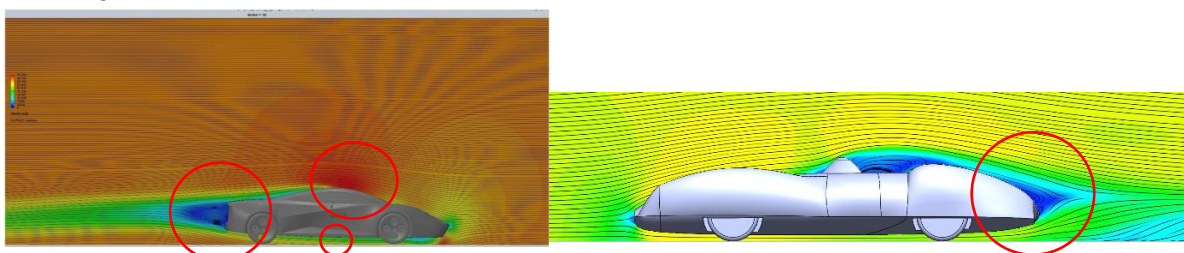**Velocity Plot Comparison:**



*Figure 12: Velocity plots of two cars*

Firstly, the curved windshield on the sports car leads to the formation of a high-speed area on the roof and a low-speed area underneath. This pressure difference between the two regions generates an apparent lift force, consequently reducing the overall downforce. Secondly, the sports car has less significant flow separation at the rear, and the convergence of upper and lower airflows at the rear is much better than the concept car. Despite the presence of some recirculation zone, the drag force remains relatively low.

Since the sports car are not convertible, there is no turbulence formed at the top area of the vehicle, resulting in a smaller drag force.
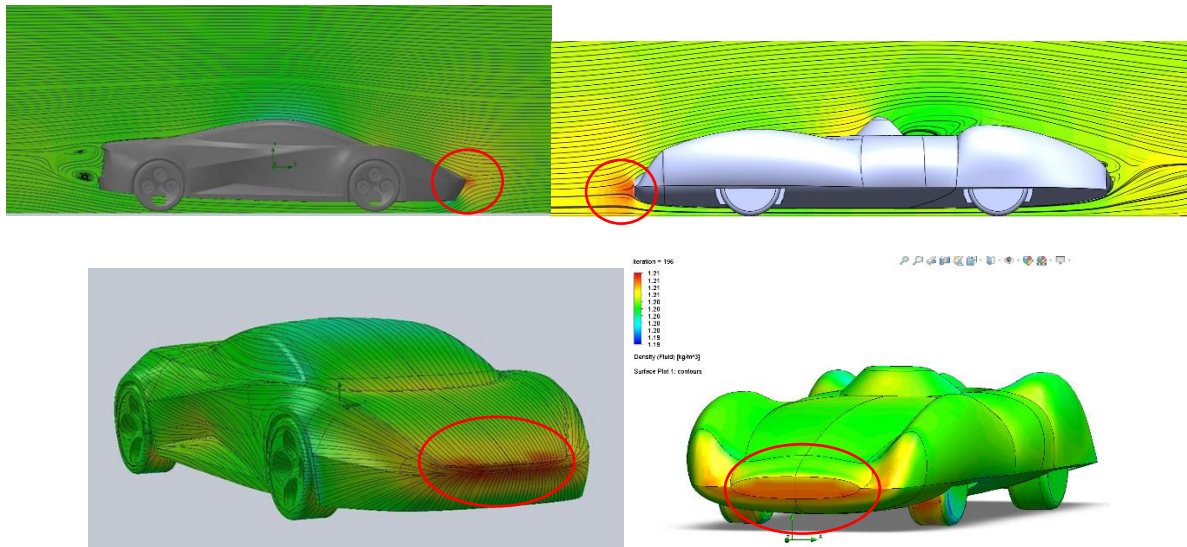
**Pressure Plot Comparison:**



*Figure 13: 2D and 3D pressure plots of two cars*

Regarding pressure plots, the performance of both vehicles is quite similar and commendable. No distinct low-pressure regions have emerged, with only a minor presence of high-pressure areas detected at their front ends. This phenomenon contributes to the drag forces experienced by both vehicles.

**Result Comparison:**

| Goal Name | Unit | Concept Car | Sports Car |
|---|---|---|---|
| Velocity | [m/s] | -31.29 | -30.83 |
| Lift Force | [N] | -7.278 | 0.983 |
| Drag Force | [N] | -260.8 | -0.966 |
| Drag Coefficient | [] | 0.3815 | 0.2719 |

*Table 4: Results Comparison between two cars*

In instances of proximate velocities, the distinct body structures and dimensions of the two cars contribute to significant variations in lift force as depicted in the pressure plots. A closer examination of the velocity plot reveals the superior aerodynamic design at the rear of the sports car, characterized by minimal flow separation and fewer vortices. As a result, the sports car encounters diminished drag force, resulting in a lower drag coefficient.
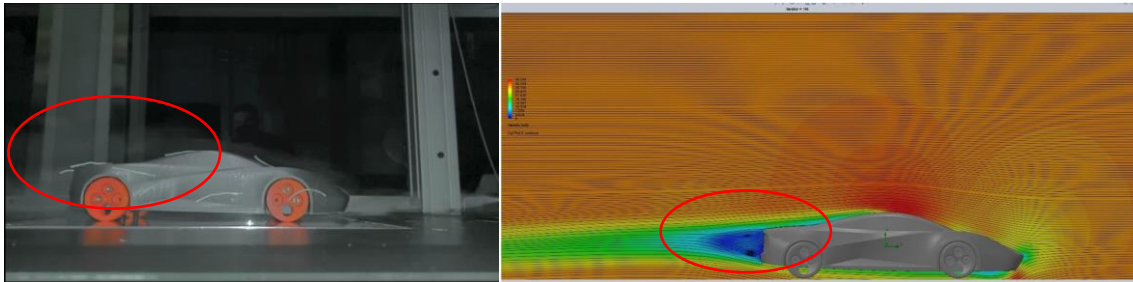
*Figure 14: Wind Tunnel Test and CFD Simulation*

| Goal Name | Unit | Wind Tunnel | CFD |
|---|---|---|---|
| Velocity | [m/s] | -30.552 | -30.83 |
| Lift Force | [N] | 1.316 | 0.983 |
| Drag Coefficient | [] | 0.37 | 0.2719 |

*Table 5: Results Comparison between wind tunnel and CFD*

In the wind tunnel test, observations revealed that flow separation was not in an ideal state, and the airflows did not perfectly adhere to the vehicle's surface. As a result, a larger recirculation zone was generated at the rear compared to what was simulated in CFD. Therefore, the drag force experienced by the sports car was actually greater than the simulated value. Additionally, the accuracy of the printed model and a series of errors introduced during the wind tunnel test setup can also lead to differences in drag coefficients between the two methods.

# 7 Improvements

After the CFD simulation and analysis, there are still a lot of structures that can be improved. In reality, the design of a race car should make a balance between a lower drag coefficient and a larger downforce. Extreme developments in either direction often imply lower stability and higher risks. The drag coefficient of the concept car is 0.3815, which is good among F1 cars, thus the improvements should focus on increasing downforce to improve the car's handling and slightly decreasing the air drag coefficient.
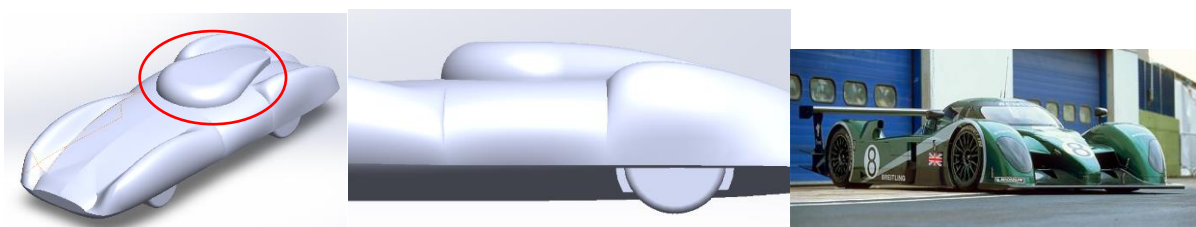
**Addition of a windshield**



*Figure 15: Remodel of the windshield [4]*

By adding a higher windshield, the car is transformed into a closed-top car. Although closed-top race cars are prevalent in Le Mans, they are not considered safe in Formula 1. However, if we only focus on addressing turbulence issues in the cabin, this method is relatively effective. And also, this can effectively reduce flow separation. (Shown in Appendix)

## Installation of a fan diffuser



Installing a fan diffuser at the rear of the car to accelerate the air passing underneath it, creating a low-pressure zone. This can significantly enhance the downforce of the race car. However, this method has already been banned in Formula 1.
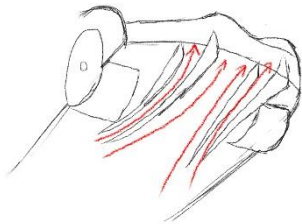
*Figure 16: 1978 Brabham BT46B [5]*

## Underbody Diffuser



Adding diffusers under the car is aimed at managing the airflow around the wheels, preventing air from being drawn into the wheel arches and causing turbulence. Simultaneously, it can reduce the vortices formed at the rear, thereby decreasing drag.
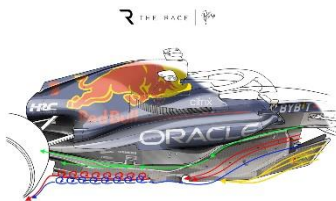
*Figure 17: Sketch of diffusers*

## Side Skirts



Side skirts not only help streamline the airflow along the sides of the car but also assist in controlling the air beneath the car, increasing the downforce.

*Figure 18: Redbull Side Skirt [6]*

## Flat and Lower Underbody
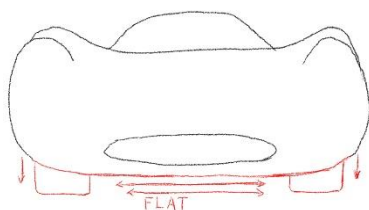


Reverting the underbody to a flat plane and lowering the chassis. A flat underbody helps reduce turbulence underneath and vortices at the rear. Additionally, the lowered chassis, combined with side skirts, creates a low-pressure zone beneath the car, thereby enhancing downforce.

*Figure 19: Changes on underbody*

# 8 Reference

[1] Thermo-Fluids: Energy and Design - Worksheet 4: CFD Drag Tutorial Sheet By Dr.Kamyar Hazeri.

[2] By (2018) *An introduction to automobile aerodynamics*, *Mechanix Illustrated*. Available at: https://mechanixillustrated.technicacuriosa.com/2017/03/04/an-introduction-to-automobile-aerodynamics/ (Accessed: 22 February 2024).

[3] SolidWorks Flow Simulation Project Report Sports car model report by Dr.Kamyar Hazeri.

[4] *A Hundred-Year racing heritage* (no date) *Bentley Motors Website: World of Bentley:TheBentley Story: History and Heritage*. Available at: https://www.bentleymotors.com/en/world-of-bentley/the-bentley-story/history-and heritage/return-to-le-mans-2003.html (Accessed: 22 February 2024).

[5] Els, P. (2021) *This is why car-design guru, Gordon Murray, is a big fan of Big Fans*, *HotCars*. Available at: https://www.hotcars.com/this-is-why-cardesign-guru-gordon-murray-is-a-big-fan-of-big-fans/ (Accessed: 22 February 2024).

[6] Anderson, G. (2023) *Gary Anderson: How Red Bull's dramatic sidepod design works*, *The Race*. Available at: https://www.the-race.com/formula-1/gary-anderson-how-red-bulls-dramatic-sidepod-design-works/ (Accessed: 22 February 2024).

# Appendix

**CFD analysis after adding windshield**
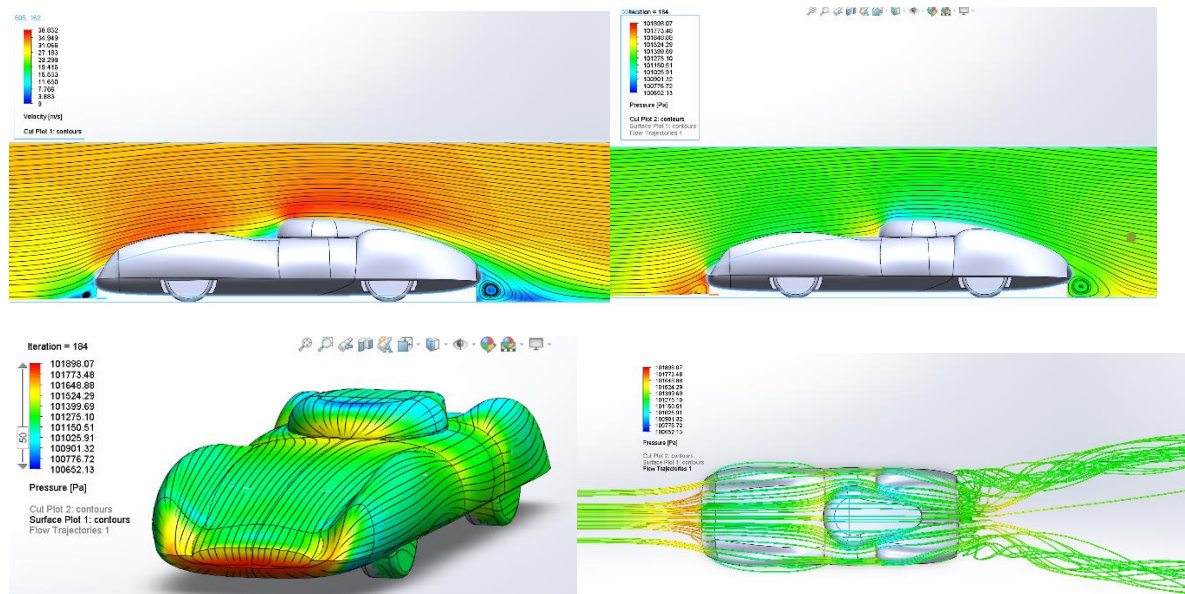


| Goal Name | Unit | Value | Progress | Use In Convergence | Delta | Criteria |
|---|---|---|---|---|---|---|
| Lift Force | [N] | 22.28 | 100 | Yes | 9.668 | 10.14 |
| Drag Force | [N] | -203.2 | 100 | Yes | 3.887 | 17.66 |
| Drag Coefficient | [] | 0.2754 | 100 | Yes | 0.0053 | 0.0239 |